PERGAMON

International Journal of Solids and Structures 39 (2002) 637–648

INTERNATIONAL JOURNAL OF SOLIDS and STRUCTURES

www.elsevier.com/locate/ijsolstr

Modelling of inherent anisotropy in sedimentary rocks

S. Pietruszczak [a,*], D. Lydzba [b], J.F. Shao [c]

[a] *Department of Civil Engineering and Engineering Mechanics, McMaster University, 1280 Main Street West, Hamilton, Ontario, Canada L8S 4L7*

[b] *Institute of Geotechnics, Technical University of Wroclaw, 50–377 Wroclaw, Poland*

[c] *EUDIL-USTL, Laboratoire de Mecanique de Lille, 59655 Villeneuve d'Ascq, France*

Received 26 September 2000; received in revised form 5 April 2001

Abstract

This paper presents a constitutive relation for modelling the inelastic response of sedimentary rocks. The inherent anisotropy of this class of materials is described by employing a second-order microstructure tensor, whose eigenvectors define the principal material triad. Higher-order dyadic products of this tensor are incorporated in the distribution function, which specifies the directional dependence of strength parameters. The mathematical formulation is applied to model the mechanical characteristics of Tournemire shale. Several triaxial tests are simulated, at various initial confining pressures, for samples tested at different orientation relative to the loading direction. The results are compared with the available experimental data. © 2002 Elsevier Science Ltd. All rights reserved.

Keywords: Inherent anisotropy; Microstructure tensor; Sedimentary rocks; Plasticity

1. Introduction

Among sedimentary rocks, the most widespread are shale, siltstone and claystone. These rocks, which are formed by deposits of clay and silt sediment, exhibit strong inherent anisotropy, manifesting itself in a directional dependence of deformation characteristics. The anisotropy is strongly related to the microstructure, in particular the existence of bedding planes which mark the limits of strata and can be easily identified by a visual examination. The study of the mechanical behaviour of sedimentary rocks, especially shale and mudstone, is of particular interest to the oil exploration industry as well as to civil and mining engineering. These materials are often unavoidable in foundations of a broad range of civil structures, in underground excavations as well as tunnelling.

Over the last few decades, an extensive research effort has been devoted to study the mechanical behaviour of anisotropic rocks. Comprehensive references on this topic can be found in a number of review papers (see e.g., Amadei (1983), Kwasniewski (1993) and Ramamurthy (1993)). One significant direction of

* Corresponding author. Tel.: +1-905-525-9140; fax: +1-905-529-9688.
E-mail address: pietrusz@mcmaster.ca (S. Pietruszczak).

0020-7683/02/$ - see front matter
PII: S0020-7683(01)00110-X

research has been that involving the experimental component. In general, several experimental studies were carried out (cf. Donath (1961), McLamore and Gray (1967), Hoek (1968), Atwell and Sandford (1974), Lerau et al. (1981) and Hoek (1983)) and the main focus was the directional dependence of rock strength. The results generally indicate that the maximum axial compressive strength is associated with configurations in which the bedding planes are either parallel or perpendicular to the loading direction. At the same time, the minimum strength is typically associated with failure along the weakness plane, which corresponds to sample orientations within the range 30–60°.

In parallel with experimental studies, extensive research has been carried out on formulation of appropriate general failure criteria. An extensive review on this topic, examining different approaches, is provided in the article by Duveau et al. (1998). In general, relatively little work has been done on the description of progressive failure in this class of materials, which stems primarily from difficulties associated with the formulation of the problem. The rigorous approach, based on general representation theorems for tensorial functions (Boehler and Sawczuk, 1970, 1977), is very complex and has never been applied to any practical problem.

The objective of this paper is to propose an approach which retains the mathematical rigour and, at the same time, is pragmatic, i.e. simple enough to be applied to solve some practical engineering problems. The formulation incorporates a scalar anisotropy parameter which is expressed in terms of mixed invariants of the stress and structure-orientation tensors. Such a parameter has recently been introduced by Pietruszczak and Mroz (2001) in the context of specification of the conditions at failure. The main focus of this work is on constructing a complete plasticity framework for describing the deformation process in anisotropic sedimentary rocks. In the next section, the formulation of the problem is outlined, followed by a discussion on the identification of material functions involved. The formulation is applied to study the behaviour of Tournemire shale. In particular, several triaxial tests are simulated at different initial confining pressures. The emphasis is on modelling of the dependence of deformation characteristics on the orientation of the sample relative to the direction of loading.

2. A constitutive model for anisotropic rocks

Consider first the specification of the conditions at failure. Following the framework developed in Pietruszczak and Mroz (2001), assume that the failure criterion can be expressed in a simplified form

$$F = F(\boldsymbol{\sigma}, \boldsymbol{a}) = F(\mathrm{tr}\,\boldsymbol{\sigma}, \mathrm{tr}\,\boldsymbol{\sigma}^2, \mathrm{tr}\,\boldsymbol{\sigma}^3, \eta) = 0 \tag{1}$$

In the above equation, $\boldsymbol{a}$ is a microstructure tensor and η is a scalar anisotropy parameter which represents the projection of this tensor on a suitably defined loading direction $\boldsymbol{l}$, i.e.

$$\eta = a_{ij} l_i l_j \tag{2}$$

In order to define the loading vector $\boldsymbol{l}$, consider the principal triad $\boldsymbol{e}^{(i)}$, $i = 1, 2, 3$, of the microstructure tensor $\boldsymbol{a}$ and specify the traction moduli on the planes normal to the principal axes

$$L_1 = (\sigma_{11}^2 + \sigma_{12}^2 + \sigma_{13}^2)^{1/2}; \qquad L_2 = (\sigma_{12}^2 + \sigma_{22}^2 + \sigma_{23}^2)^{1/2}; \qquad L_3 = (\sigma_{13}^2 + \sigma_{23}^2 + \sigma_{33}^2)^{1/2} \tag{3}$$

The generalized loading vector $\boldsymbol{l}$ is now defined as

$$l_i = \frac{L_i}{(L_k L_k)^{1/2}}; \qquad L_i = L_1 e_i^{(1)} + L_2 e_i^{(2)} + L_3 e_i^{(3)} \tag{4}$$

It can be shown (see Pietruszczak and Mroz (2001)) that the traction moduli (3) can be expressed as mixed invariants of the stress and structure-orientation tensors, so that the projection of $\boldsymbol{a}$ on the direction $\boldsymbol{l}$ becomes

$$\eta = a_{ij} l_i l_j = \frac{\mathrm{tr}(\boldsymbol{a}\boldsymbol{\sigma}^2)}{\mathrm{tr}\,\boldsymbol{\sigma}^2} \tag{5}$$

Thus, the anisotropy parameter η specifies the effect of load orientation relative to material axes and is expressed as the ratio of the joint invariant to the second stress invariant. It is a homogeneous function of stress of the degree zero, so that the stress magnitude does not affect its value.

Another way of expressing the definition (5) is to employ the deviatoric part A of the microstructure tensor, so that

$$\eta = \hat{\eta}(1 + A_{ij} l_i l_j); \qquad A_{ij} = (a_{ij} - \hat{\eta}\delta_{ij})/\hat{\eta}; \qquad \hat{\eta} = \tfrac{1}{3} a_{kk} \tag{6}$$

The above distribution function is similar to that employed by Kanatani (1984). Here, A is a traceless symmetric tensor describing the bias in the spatial distribution of $\eta(\boldsymbol{l})$ with respect to the mean value $\hat{\eta}$. A more general expression for η can be obtained by including higher-order tensors

$$\eta = \hat{\eta}(1 + A_{ij} l_i l_j + A_{ijkl} l_i l_j l_k l_l + A_{ijklmn} l_i l_j l_k l_l l_m l_n + \cdots) \tag{7}$$

A special case of this representation, which is pursued further in this paper, corresponds to introducing dyadic products of A, i.e. $A_{ijkl} = b_1 A_{ij} A_{kl}$; $A_{ijklmn} = b_2 A_{ij} A_{kl} A_{mn}$, etc., so that

$$\eta = \hat{\eta}[1 + A_{ij} l_i l_j + b_1 (A_{ij} l_i l_j)^2 + b_2 (A_{ij} l_i l_j)^3 + \cdots] \tag{8}$$

With the notion of anisotropy parameter η, as defined above, let us turn our attention now to the description of inelastic properties of sedimentary rocks. In general, the problem can be formulated within the framework of elastoplasticity by assuming the yield criterion in the form

$$f = f(\boldsymbol{\sigma}, \boldsymbol{a}, \boldsymbol{\varepsilon}^{\mathrm{p}}) = f(\mathrm{tr}\,\boldsymbol{\sigma}, \mathrm{tr}\,\boldsymbol{\sigma}^2, \mathrm{tr}\,\boldsymbol{\sigma}^3, \eta, \beta) = 0 \tag{9}$$

In Eq. (9), β is a scalar-valued function of plastic deformation. The flow rule may now be written as

$$\mathrm{d}\varepsilon^{\mathrm{p}}_{ij} = \mathrm{d}\lambda \frac{\partial \psi}{\partial \sigma_{ij}}; \qquad \psi = \psi(\mathrm{tr}\,\boldsymbol{\sigma}, \mathrm{tr}\,\boldsymbol{\sigma}^2, \mathrm{tr}\,\boldsymbol{\sigma}^3, \eta) \tag{10}$$

where $\psi = \text{const.}$ is the plastic potential.

A specific formulation can be obtained by a suitable generalization of classical isotropic criteria. Consider, for this purpose, the plasticity framework for brittle-plastic materials as outlined in the article by Pietruszczak et al. (1988). Assume that the conditions at failure can be described by employing a quadratic form

$$F = c_1 \left(\frac{\overline{\sigma}}{g(\theta) f_{\mathrm{c}}} \right) + c_2 \left(\frac{\overline{\sigma}}{g(\theta) f_{\mathrm{c}}} \right)^2 - \left(c_3 + \frac{I}{f_{\mathrm{c}}} \right) = 0 \tag{11}$$

In the equation above, $\overline{\sigma} = J_2^{1/2} = (\mathrm{tr}\,\boldsymbol{s}^2)^{1/2}$, $I = -\mathrm{tr}\,\boldsymbol{\sigma}$, $\theta = (1/3)\sin^{-1}(-3\sqrt{3}J_3/2\overline{\sigma}^3)$ and $\boldsymbol{s}$ is the stress deviator. The parameter θ represents Lode's angle and is defined within the interval $-\pi/6 \leqslant \theta \leqslant \pi/6$, while $g(\theta)$ satisfies $g(\pi/6) = 1$, $g(-\pi/6) = K$, where K is a constant. Moreover, c's are material constants and f_{c} represents the uniaxial compressive strength. For an isotropic material $f_{\mathrm{c}} = \text{const.}$ and the criterion (11) is path independent. In order to account for inherent anisotropy, assume that f_{c} is affected by the orientation of the sample and describe its variation by incorporating a distribution function similar to Eq. (8), i.e.

$$f_{\mathrm{c}} = \hat{f}[1 + A_{ij} l_i l_j + b_1 (A_{ij} l_i l_j)^2 + b_2 (A_{ij} l_i l_j)^3 + \cdots] \tag{12}$$

Thus, the anisotropy parameter η, appearing in the general form of the failure criterion (1), is now explicitly identified with f_{c}. Moreover, since the value of f_{c} depends on the relative orientation of both the stress and microstructure tensors, the representation (12) implies the path dependency of Eq. (11).

For further analysis, it is convenient to express Eq. (11) in the form

$$F = \overline{\sigma} - g(\theta)\overline{\sigma}_c = 0; \qquad \overline{\sigma}_c = \frac{-c_1 + \sqrt{(c_1^2 + 4c_2(c_3 + I/f_c))}}{2c_2} f_c \tag{13}$$

The yield function may now be assumed in a functional form similar to Eq. (13), i.e.

$$f = \overline{\sigma} - \beta(\xi)g(\theta)\overline{\sigma}_c = 0 \tag{14}$$

Here, $\beta \subseteq (0,1)$ is a hardening function, and ξ is a suitably chosen damage parameter. Restricting the considerations to the ductile regime, the function β can be selected in a simple hyperbolic form

$$\beta(\xi) = \frac{\xi}{B + \xi}; \qquad \mathrm{d}\xi = (\mathrm{d}e_{ij}^{\mathrm{p}}\,\mathrm{d}e_{ij}^{\mathrm{p}})^{1/2}; \qquad \xi = \int \mathrm{d}\xi \tag{15}$$

where B is a material constant and e represents the strain deviator. It should be noted that in view of Eqs. (15) and (12), the functional form of the yield criterion is consistent with representation (9).

The plastic multiplier $\mathrm{d}\lambda$, Eq. (10), can be determined from the consistency condition $\mathrm{d}f = 0$. Thus,

$$\mathrm{d}\lambda = H^{-1}\frac{\partial f}{\partial \sigma_{ij}}\mathrm{d}\sigma_{ij}; \qquad H = -\frac{\partial f}{\partial \beta}\frac{\mathrm{d}\beta}{\mathrm{d}\xi}\left(\mathrm{dev}\frac{\partial \psi}{\partial \sigma_{ij}}\mathrm{dev}\frac{\partial \psi}{\partial \sigma_{ij}}\right)^{1/2} \tag{16}$$

where H is the plastic hardening modulus. For the functional form (14), the gradient tensor can be expressed as

$$\frac{\partial f}{\partial \sigma_{ij}} = \left(\frac{\partial f}{\partial I}\frac{\partial I}{\partial \sigma_{ij}} + \frac{\partial f}{\partial \overline{\sigma}}\frac{\partial \overline{\sigma}}{\partial \sigma_{ij}} + \frac{\partial f}{\partial \theta}\frac{\partial \theta}{\partial \sigma_{ij}}\right) + \left(\frac{\partial f}{\partial f_c}\frac{\partial f_c}{\partial \sigma_{ij}}\right) \tag{17}$$

where

$$\frac{\partial I}{\partial \sigma_{ij}} = -\delta_{ij}; \qquad \frac{\partial \overline{\sigma}}{\partial \sigma_{ij}} = \frac{1}{2\overline{\sigma}}s_{ij}; \qquad \frac{\partial \theta}{\partial \sigma_{ij}} = \frac{\sqrt{3}}{2\overline{\sigma}^3\cos 3\theta}\left(\frac{3J_3}{2\overline{\sigma}^2}s_{ij} - s_{ik}s_{kj} + \frac{2}{3}\overline{\sigma}^2\delta_{ij}\right) \tag{18}$$

It is evident, from Eq. (17), that the effect of anisotropy is embedded in the last term appearing in this expression. In order to evaluate this term, note that according to Eq. (14),

$$\frac{\partial f}{\partial f_c} = -\beta(\xi)g(\theta)\left(\frac{\overline{\sigma}_c}{f_c} - \frac{I}{2c_2\overline{\sigma}_c + c_1 f_c}\right) \tag{19}$$

whereas

$$\frac{\partial f_c}{\partial \sigma_{ij}} = \frac{\partial f_c}{\partial \zeta}\frac{\partial \zeta}{\partial \sigma_{ij}}; \qquad \zeta = A_{pq}l_p l_q = \frac{\mathrm{tr}(\boldsymbol{A}\boldsymbol{\sigma}^2)}{\mathrm{tr}(\boldsymbol{\sigma}^2)} = \frac{A_{pk}\sigma_{pq}\sigma_{kq}}{\sigma_{mn}\sigma_{mn}} \tag{20}$$

Substituting for f_c from Eq. (12), and differentiating, one obtains

$$\frac{\partial f_c}{\partial \sigma_{ij}} = 2\hat{f}(1 + 2b_1\zeta + 3b_2\zeta^2 + \cdots)\frac{A_{ki}\sigma_{kj}\sigma_{pq}\sigma_{pq} - A_{pk}\sigma_{pq}\sigma_{kq}\sigma_{ij}}{(\sigma_{mn}\sigma_{mn})^2} \tag{21}$$

which completes the evaluation of the gradient term (17), and thus $\mathrm{d}\lambda$ in Eq. (16).

The final aspect of the formulation of the problem is the specification of the plastic potential function. The experimental evidence indicates that in the ductile regime a significant dilation takes place prior to failure. In order to account for this effect, the plastic potential may be assumed in the form

$$\psi = \overline{\sigma} + \eta_c g(\theta)\overline{I}\ln(\overline{I}/\overline{I}_o) = 0 \tag{22}$$

where $\overline{I} = c_3 f_c + I$ and η_c represents the value of $\overline{\sigma}/(g(\theta)\overline{I})$ at which the transition from compaction to dilatancy occurs. Assuming that such a transition takes place along the locus

$$\overline{\sigma} - \upsilon g(\theta)\overline{\sigma}_c = 0 \tag{23}$$

where υ is a material constant, one can define η_c as (cf. Pietruszczak et al. (1988))

$$\eta_c = \frac{\upsilon e f_c}{2c_2\bar{I}_o}(d - c_1); \qquad d = \sqrt{c_1^2 + \frac{4c_2}{e f_c}\bar{I}_o} \tag{24}$$

It is evident from Eq. (24) that η_c depends on f_c, so that the functional form (22) is consistent with representation (10). Thus, the direction of plastic flow is defined by

$$\frac{\partial\psi}{\partial\sigma_{ij}} = \left(\frac{\partial\psi}{\partial I}\frac{\partial I}{\partial\sigma_{ij}} + \frac{\partial\psi}{\partial\overline{\sigma}}\frac{\partial\overline{\sigma}}{\partial\sigma_{ij}} + \frac{\partial\psi}{\partial\theta}\frac{\partial\theta}{\partial\sigma_{ij}}\right) + \left(\frac{\partial\psi}{\partial f_c}\frac{\partial f_c}{\partial\sigma_{ij}}\right) \tag{25}$$

Once again, the effect of anisotropy is embedded in the last term appearing in Eq. (25). Given Eq. (22),

$$\frac{\partial\psi}{\partial f_c} = -\frac{\overline{\sigma}}{\eta_c}\frac{\partial\eta_c}{\partial f_c} + \eta_c g(\theta)c_3 - \frac{c_3\overline{\sigma}}{c_3 f_c + I} \tag{26}$$

whereas from Eq. (24)

$$\frac{\partial\eta_c}{\partial f_c} = \frac{\upsilon e}{2c_2\bar{I}_o}(d - c_1) + \frac{\upsilon}{f_c d} \tag{27}$$

which together with Eqs. (18) and (21) completely defines the gradient tensor (25).

Given the gradients of both the yield and plastic potential functions, the constitutive relation can be evaluated by employing a standard plasticity procedure. Assuming the additivity of elastic and plastic strain rates, and employing the definition (16), one obtains

$$\mathrm{d}\sigma_{ij} = \left[D^e_{ijkl} - \frac{1}{\overline{H}}\left(D^e_{ijpq}\frac{\partial\psi}{\partial\sigma_{pq}}\frac{\partial f}{\partial\sigma_{mn}}D^e_{mnkl}\right)\right]\mathrm{d}\varepsilon_{kl}; \qquad \overline{H} = H + \frac{\partial f}{\partial\sigma_{pq}}D^e_{pqrs}\frac{\partial\psi}{\partial\sigma_{rs}} \tag{28}$$

where H is defined in Eq. (16) and D^e_{ijkl} is the elastic stiffness. It is noted that the elastic properties should, in general, reflect the form of anisotropy implied by the microstructure tensor a_{ij}, and thus A_{ij}.

Finally, it should be emphasized that the formulation presented here is restricted to ductile regime. This is implied by the form of the hardening law (15). In general, the inception of localized deformation may be considered as a bifurcation problem (Rudnicki and Rice, 1975). Subsequent behaviour, which is typically associated with strain softening, may be described by following, for example, a homogenization procedure similar to that developed in Pietruszczak and Xu (1995) or Pietruszczak (1999).

3. On identification of material functions/parameters

The formulation outlined in the previous section has been applied to model the mechanical characteristics of a shale taken from the Tournemire site in the Massif Central, France. A comprehensive experimental program has been carried out at Laboratoire de Mécanique de Lille, and the results have been reported by Niandou (1994) and Niandou et al. (1997). The primary minerals for this shale are kaolinite (27.5%), quartz (19%), illite (16.5%) and calcite (15%) and the porosity is in the range of 8%. The material exhibits an inherent transverse isotropy, due to the presence of a set of bedding planes.

In general, the implementation of the constitutive relation (28) requires the specification of material functions and parameters involved, especially those associated with the distribution function (12), as well as the failure criterion (11). Consider first the function (12), which describes the variation of uniaxial compressive strength f_c. The relevant experimental data (after Niandou (1994)) is provided in Fig. 1, which shows the variation of f_c with the orientation of bedding planes, the latter measured in terms of the angle α.

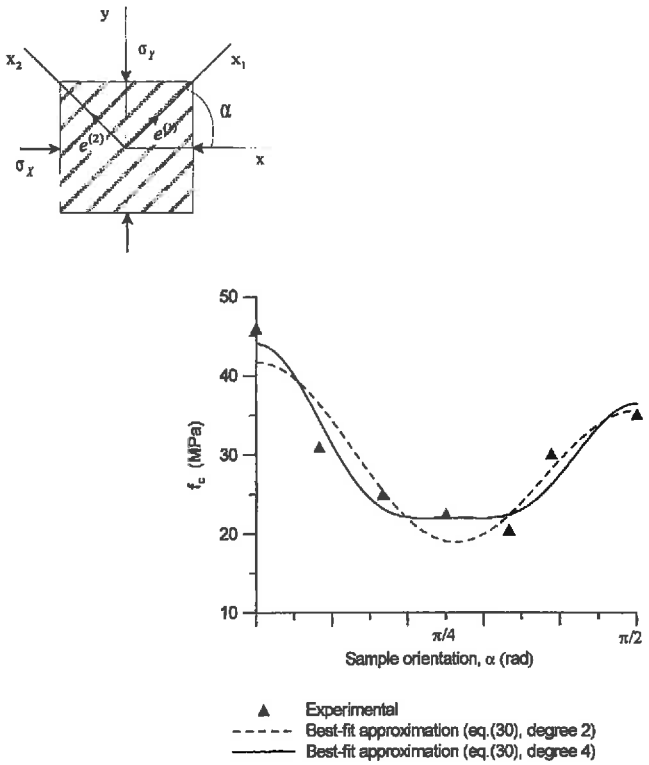

Fig. 1. Variation of uniaxial compressive strength, f_c, with sample orientation, α.

It is evident that the strength is the highest for $\alpha = 0$, i.e. when the loading direction is orthogonal to the bedding planes. At the same time, for $\alpha \approx 60°$ the strength is reduced by over 50%.

In order to approximate the data by the distribution function (12), let us note that for the considered loading process ($\sigma_x = \sigma_z = 0$; $\sigma_y = \sigma_1 < 0$) and the type of anisotropy ($A_1 = A_3 = -0.5\, A_2$), there is

$$A_{ij} l_i l_j = A_1(1 - 3l_2^2); \qquad l_2^2 = \cos^2\alpha \tag{29}$$

so that

$$f_c = \hat{f}[1 + A_1(1 - 3\cos^2\alpha) + b_1 A_1^2(1 - 3\cos^2\alpha)^2 + b_2 A_1^3(1 - 3\cos^2\alpha)^3 + b_3 A_1^4(1 - 3\cos^2\alpha)^4 + \cdots] \tag{30}$$

The best-fit approximations, employing representation (30) are shown in Fig. 1. The results correspond to approximations incorporating the dyadic products of up to degree 2 (i.e., $b_2 = b_3 = \cdots 0$) and 4, respectively. From the experimental data itself, it is evident that a simple linear representation, based on Eq. (6), is not adequate here. A reasonable approximation is obtained by incorporating the terms up to order 4 in Eq. (30), and corresponds to

$$A_1 = 0.0170251; \quad \hat{f} = 22 \text{ MPa}; \quad b_1 = 515.49; \quad b_2 = 61\,735.3; \quad b_3 = 2\,139\,820.0 \tag{31}$$

The next issue is that of identification of the constants appearing in the failure criterion (11). For this purpose, the results of triaxial tests at different initial confining pressures, as reported by Niandou (1994),

have been utilized. In particular, it has been assumed that the ultimate strength, for $\alpha = 0$, is attained at the following stress conditions

$$\{\sigma_x = \sigma_z, \sigma_y\} = \{-50, -155\};\ \{-40, -130\};\ \{-20, -100\};\ \{-5, -55\};\ \{0, -46\};\ \{4.6, 4.6\} \tag{32}$$

In the above expressions, $\sigma_x = \sigma_z$ specifies the magnitude of confining pressure (kept constant during each test), whereas σ_y is the maximum vertical stress attained; the units are MPa. It is noted that the considered loading program corresponds to $\theta = \pi/6$; $g(\pi/6) = 1$ in Eq. (11), so that

$$\frac{I}{f_c} = -c_3 + c_1\left(\frac{\bar{\sigma}}{f_c}\right) + c_2\left(\frac{\bar{\sigma}}{f_c}\right)^2 \tag{33}$$

where $I = -(\sigma_y + 2\sigma_x)$; $\sqrt{3}\bar{\sigma} = \sigma_x - \sigma_y$. Moreover, according to Eqs. (3) and (4),

$$l_1 = \sigma_x \Big/ \sqrt{2\sigma_x^2 + \sigma_y^2}; \qquad l_2 = \sigma_y \Big/ \sqrt{2\sigma_x^2 + \sigma_y^2}; \qquad l_3 = l_1 \tag{34}$$

so that

$$f_c = \hat{f}(1 + \zeta + b_1\zeta^2 + b_2\zeta^3 + b_3\zeta^4); \qquad \zeta = A_{ijkl}\, l_i l_j = 2A_1^2(l_1^2 - l_2^2) \tag{35}$$

where A_1, together with $\hat{f}$, b_1, b_2 and b_3 are defined in Eq. (31).

Fig. 2 shows the best-fit approximation based on the polynomial function (33). Here, the experimental data consists of a set of consecutive pairs $\{I/f_c, \bar{\sigma}/f_c\}$, evaluated based on Eqs. (32) and (35). The resulting values of the coefficients are

$$c_1 = 2.3729; \qquad c_2 = 0.9371; \qquad c_3 = 0.6582 \tag{36}$$

The elastic constants for Tournemire shale have been identified by Niandou (1994), based on a series of tests involving partial unloading of the samples. The following values have been assigned

$$E_1 = 22000 \text{ MPa}; \quad E_2 = 7000 \text{ MPa}; \quad \nu_{21} = 0.12; \quad \nu_{13} = 0.14; \quad G = 4000 \text{ MPa} \tag{37}$$

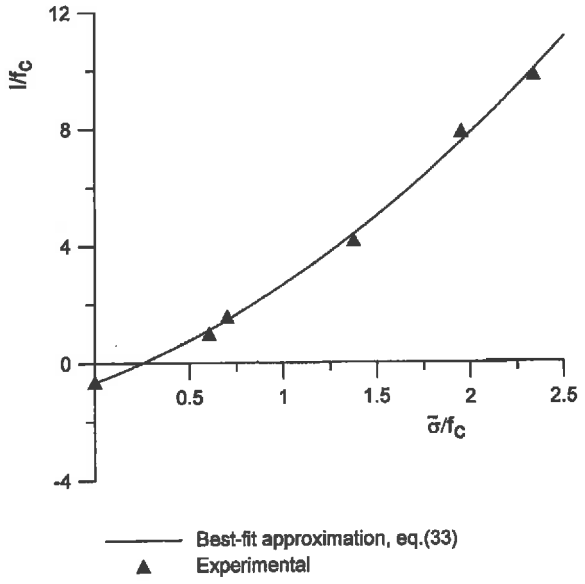

Fig. 2. Meridional section $(I/f_c, \bar{\sigma}/f_c)$ of the failure surface (11).

Finally, based on the same set of experimental results, the transition from compaction to dilatancy, Eq. (23), was assumed to occur at $v = 0.8$, whereas the constant B, Eq. (15), was given the value of 0.005. The latter was chosen based on the simulations of mechanical characteristics corresponding to $\alpha = 0$, as presented in the next section.

4. Numerical Simulations

In order to illustrate the performance of the model, a number of triaxial tests, as reported by Niandou (1994) and Niandou et al. (1997), have been simulated. The tests, carried out on Tournemire shale, involved different initial confining pressures as well as different orientations of the samples relative to the loading direction. The results of numerical simulations are provided in Figs. 3–7.

Fig. 3 shows the mechanical characteristics for vertical samples, $\alpha = 0$, tested at confining pressures ranging from 5 to 40 MPa. Fig. 3a shows the deviatoric stress against the axial deformation, whereas Fig. 3b presents the corresponding volume change characteristics. It is evident that the ultimate strength is significantly affected by the confining pressure, while the samples undergo progressive compaction prior to failure. It is noted that for this class of materials, a transition to unstable (strain softening) response, associated with strain localization, typically occurs in the range of low confining pressures. As the formulation here is restricted to hardening regime, Eq. (15), the numerical simulations were terminated at $\beta \geqslant 0.98$. The experimental data, taken from the work of Niandou (1994), also excludes the strain softening branch.

Fig. 4 shows the mechanical characteristics for inclined samples, $\alpha = 45°$. Again, the results correspond to different confining pressures, 5 and 40 MPa. In general, the axial strength is significantly lower compared

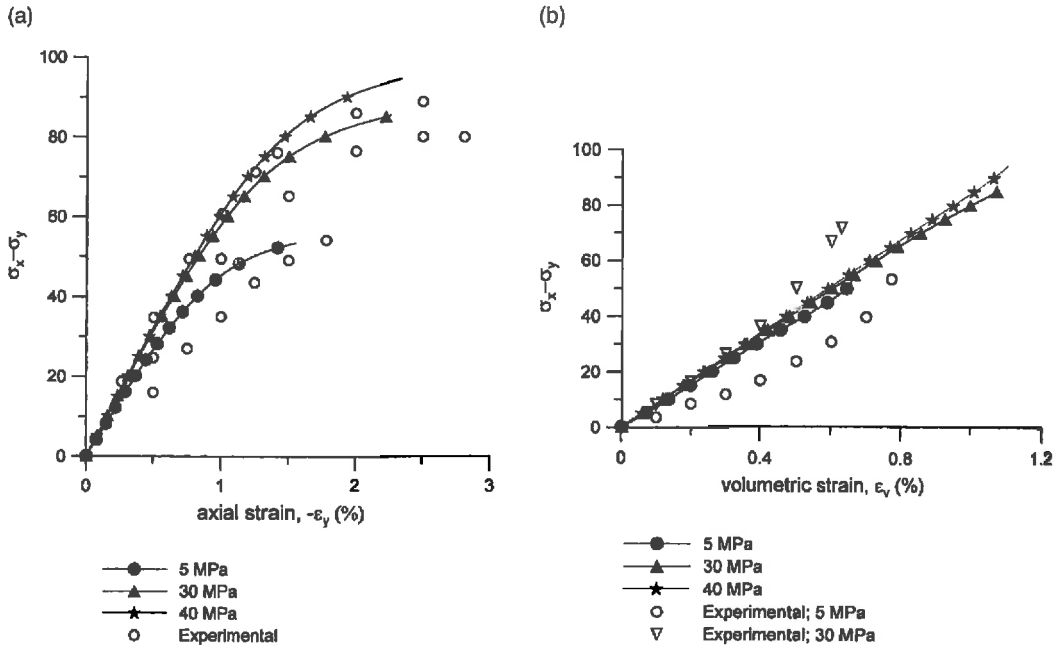

Fig. 3. Numerical simulations of triaxial tests for vertical samples, $\alpha = 0$; (a) deviatoric stress versus axial strain and (b) volume change $\varepsilon_v = -(\varepsilon_x + \varepsilon_y + \varepsilon_z)$ characteristics.

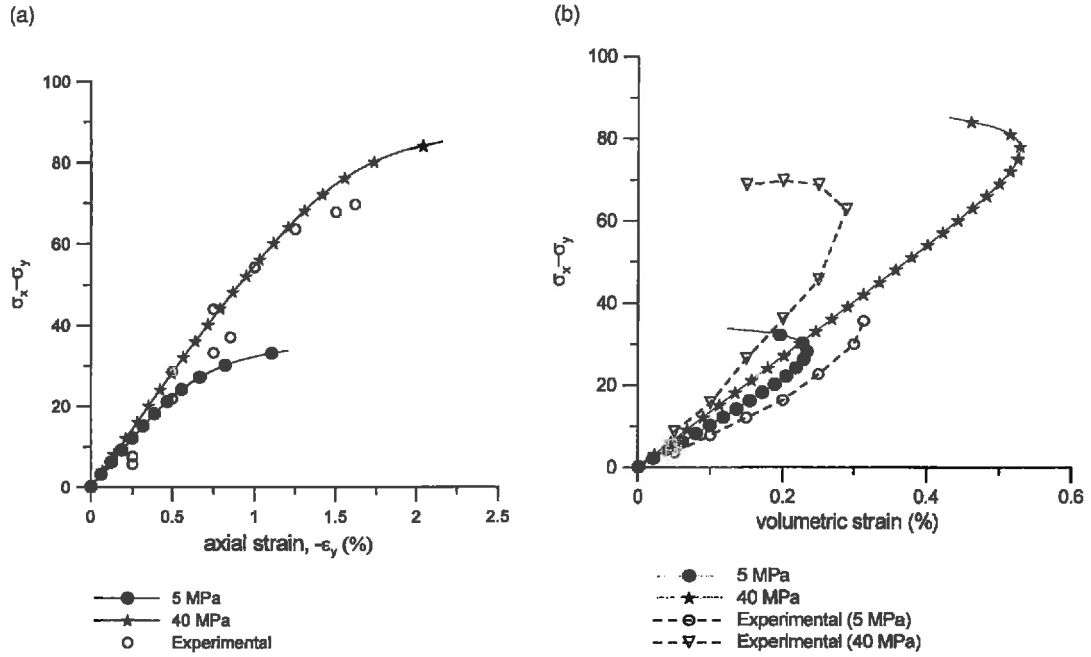

Fig. 4. Numerical simulations of triaxial tests for inclined samples, $\alpha = 45°$; (a) deviatoric stress versus axial strain and (b) volume change characteristics.

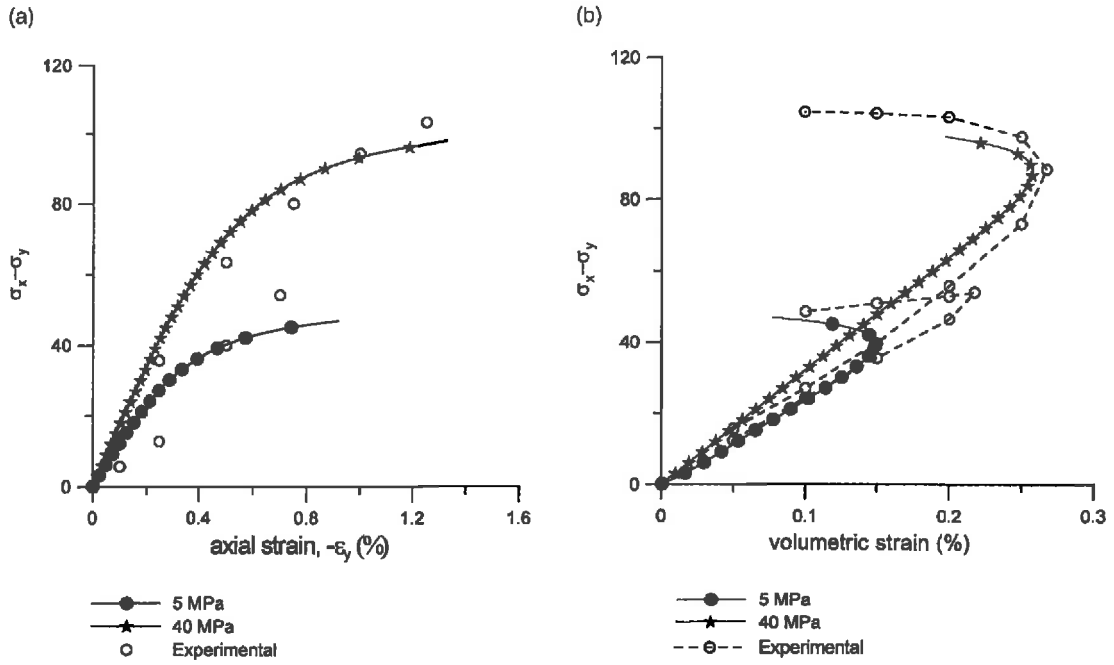

Fig. 5. Numerical simulations of triaxial tests for samples loaded in the direction of bedding planes, $\alpha = 90°$; (a) deviatoric stress versus axial strain and (b) volume change characteristics.

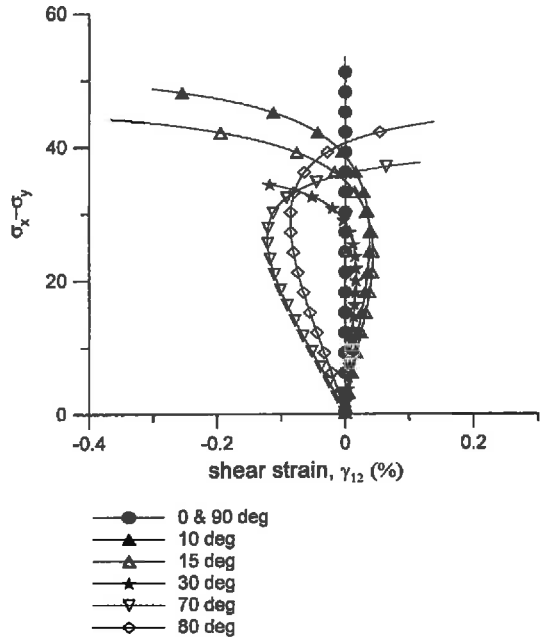

Fig. 6. Predicted generation of shear strains in samples tested at different orientations (confining pressure of 5 MPa).

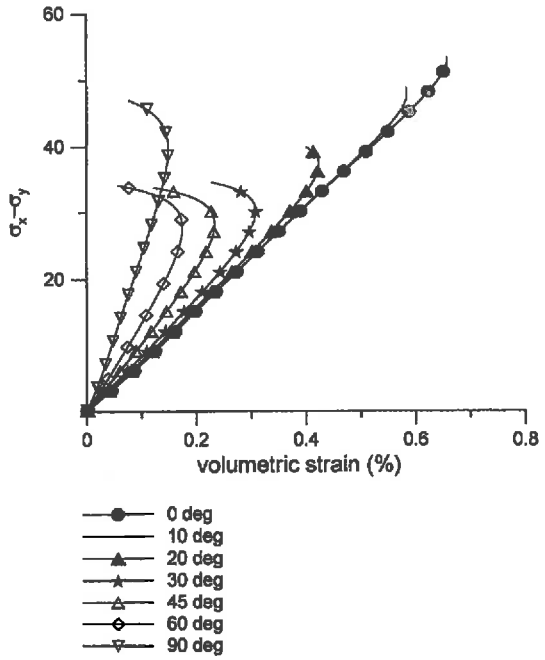

Fig. 7. Evolution of volume change with orientation of the sample (confining pressure of 5 MPa).

to that corresponding to $\alpha = 0$, Fig. 3, while the material undergoes a transition from compaction to dilatancy, Fig. 4b. Both these trends are consistent with the experimental evidence. Fig. 5 presents the same characteristics for samples at $\alpha = 90°$, i.e. when the load is in the direction of the bedding planes. General observations are similar, i.e. the strength increases in relation to samples tested at $\alpha = 45°$, while the dilatancy effects become even more pronounced.

Comparing the results in Figs. 3–5 with the experimental data, is it clear that the basic trends are quite consistent. Also, the quantitative predictions seem to be quite reasonable. It should be pointed out here that the experimental program was quite comprehensive as it involved, in addition to monotonic tests, a series of triaxial tests with complete and partial unloading. However, a close examination of the results reveals that the experimental scatter, due to inhomogeneity of the material, was quite significant, so that the quantitative aspect should indeed be regarded with caution. Moreover, it should be emphasized that in the formulation of the problem, the hardening characteristics have been described by invoking only one scalar parameter, B, Eq. (15). Apparently, a more sophisticated approach may be employed by assuming that these characteristics are affected by the confining pressure (cf. Pietruszczak et al. (1988)). The later, however, would inevitably result in a set of additional parameters/functions, thereby making the formulation less appealing.

The effects of anisotropy are discussed further in Figs. 6 and 7. In general, the numerical simulations reveal that the deformation mode remains axisymmetric only for a vertical sample ($\alpha = 0$). For $\alpha = 90°$, there is $\varepsilon_x \neq \varepsilon_z$, whereas for all inclined samples an additional generation of shear strains takes place. This is shown in Fig. 6, which presents the variation of shear strain with deviatoric stress, for a number of distinct orientations. It is noted that the distortions were not measured experimentally, so that no direct comparison could be made. Another interesting feature is the evolution of volume characteristics, as shown in Fig. 7. For the selected value of $v = 0.8$ (Section 3), an *isotropic* material will undergo a significant dilation for $\beta > v$, Eq. (23), irrespective of the orientation of the sample. This is clearly not the case here. In fact, it is evident from Fig. 7 that one of the manifestations of inherent anisotropy is the tendency to suppress the dilation for orientations close to vertical. Thus, for $0° \leqslant \alpha \leqslant 20°$ the predominant deformation mode is the compaction, while for $\alpha > 30°$, the sample dilates prior to failure. Again, these trends are consistent with the experimental evidence, as reported by Niandou et al. (1997).

5. Final remarks

In this work, a mathematical formulation has been put forth for the description of deformation characteristics of anisotropic sedimentary rocks. The primary focus was to propose an approach which is rigorous, but at the same time is simple enough to be implemented for the solution of practical engineering problems. The framework has been illustrated by numerical examples simulating a series of triaxial tests carried out on Tournemire shale. It appears that the basic trends in mechanical characteristics, i.e. sensitivity of the axial strength, axial deformation and volume change to the orientation of the sample, have been predicted quite reasonably. Also, the quantitative predictions are fairly consistent with the experimental evidence, especially given the uncertainty associated with inhomogeneity of the material.

For materials displaying a strong inherent anisotropy, the principal material directions are known a priori. Thus, the problem does not require any specific measure of fabric. This is not the case, however, in the context of induced anisotropy. The latter requires, in addition to an explicit definition of fabric, an appropriate evolution law for the fabric tensor. This issue is relevant to a broad class of rocks, including sandstone, porous chalk, etc., and will be addressed separately.

References

Amadei, B., 1983. Rock Anisotropy and the Theory of Stress Measurements. Springer, Berlin.

Atwell, P.B., Sandford, M.A., 1974. Intrinsic shear strength of a brittle anisotropic rock – I: experimental and mechanical interpretation. Int. J. Rock Mech. Min. Sci. Geomech. Abstr. 11, 423–430.

Boehler, J.P., Sawczuk, A., 1970. Equilibre limite des sols anisotropes. J. de Mécanique 3, 5–33.

Boehler, J.P., Sawczuk, A., 1977. On yielding of oriented solids. Acta Mechanica 27, 185–206.

Donath, F.A., 1961. Experimental study of shear failure in anisotropic rocks. Geol. Soc. Am. Bull. 72, 985–990.

Duveau, G., Shao, J.F., Henry, J.P., 1998. Assessment of some failure criteria for strongly anisotropic materials. Mech. Cohesive Frict. Mater. 3, 1–26.

Hoek, E., 1968. Brittle failure of rock. In: Stagg, G., Zienkiewicz, O.C. (Eds.), Rock Mechanics in Engineering Practice. Wiley, London, pp. 99–124.

Hoek, E., 1983. Strength of jointed rock masses. Geotechnique 33, 187–205.

Kanatani, K., 1984. Distribution of directional data and fabric tensor. Int. J. Engng. Sci. 22, 149–161.

Kwasniewski, M.A., 1993. Mechanical behaviour of anisotropic rocks. In: Hudson, J.A. (Ed.), Comprehensive Rock Engineering, vol. 1: Fundamentals. Pergamon Press, Oxford, pp. 285–312.

Lerau, J., Saint Leu, C., Sirieys, P., 1981. Anisotrophie de la dilatance des roches schisteuses. Rock Mech. Rock Engng. 13, 185–196.

McLamore, R., Gray, K.E., 1967. The mechanical behaviour of anisotropic sedimentary rocks. J. Engng. Industry, Trans. ASME 89, 62–73.

Niandou, H., 1994. Etude du comportement rhéologique et modélisation de l'argilite de Tournemire: Applications á la stabilité d'ouvrages souterrains. Ph.D. Thesis, Université de Lille.

Niandou, H., Shao, J.F., Henry, J.P., Fourmaintraux, D., 1997. Laboratory investigation of the mechanical behaviour of Tournemire shale. Int. J. Rock Mech. Min. Sci. 34, 3–16.

Pietruszczak, S., 1999. On homogeneous and localized deformation in water-infiltrated soils. J. Damage Mech. 8, 233–253.

Pietruszczak, S., Mroz, Z., 2001. On failure criteria for anisotropic cohesive-frictional materials. Int. J. Numer. Anal. Meth. Geomech. 25, 509–524.

Pietruszczak, S., Xu, G., 1995. Brittle response of concrete as a localization problem. Int. J. Solids Struct. 32, 1517–1533.

Pietruszczak, S., Jiang, J., Mirza, F.A., 1988. An elastoplastic constitutive model for concrete. Int. J. Solids Struct. 24, 705–722.

Ramamurthy, T., 1993. Strength and modulus responses of anisotropic rocks. In: Hudson, J.A. (Ed.), Comprehensive Rock Engineering, vol. 1: Fundamentals. Pergamon Press, Oxford, pp. 319–329.

Rudnicki, J.W., Rice, J.R., 1975. Conditions for the localization of deformation in pressure-sensitive dilatant materials. J. Mech. Phys. Solids 23, 371–394.